REVISTA MATÉRIA
V.24 N.02
ISSN 1517-7076 articles e-12371, 2019

Changing the characteristics of the nitrided layer using three different plasma configurations

Clodomiro Alves Junior [1,2], Nathalia Viviane de Sousa Freitas[1], Priscila Borges de Morais[1], Jussier de Oliveira Vitoriano[2]

[1] Labplasma, Programa de pós-graduação em Ciência e Engenharia de Materiais, Universidade Federal Rural do Semiárido, R. Francisco Mota, 572 - Pres. Costa e Silva, CEP: 59625-900, Mossoró, Rio Grande do Norte, Brasil.
[2] Programa de Pós-graduação em Engenharia Mecânica, UFRN, CP:1524, CEP - 59078-970, Natal, Rio Grande do Norte, Brasil.
e-mail: clodomiro.jr@ufersa.edu.br

ABSTRACT

Direct current (DC) plasma nitriding offers some disadvantages, especially in parts with complex geometries, where the presence of edges is significant, such as gears, molds, and needle punched parts are strongly affected by this effect, leading to irregular formation of nitrided layers and high variation in surface hardness. To solve these problems two techniques were developed as alternatives, namely: pulsed plasma nitriding and cathodic cage nitriding. In this work, these three nitriding techniques were compared using AISI 1045 steel as substrate. Steel discs were nitrided with the purpose of evaluating the influence of these different plasma configurations on the characteristics of the nitrided layer. The treatments in the three techniques were carried out at the same pressure, temperature, time and gas atmosphere. The samples were characterized for the microstructure, microhardness and crystalline phases present. X-ray diffraction with grazing incidence was used to verify the order of the nitrites formed and to estimate the thickness of the single-phase layers. Differences between the configurations with respect to the occurrence of restriction rings, total thickness ($x_\varepsilon + x_{\gamma'}$) and relative ($x_\varepsilon/x_{\gamma'}$) compound layers were observed.

Keywords: Plasma DC; cathodic cage; pulsed plasma; nitriding; GIXRD.

1. INTRODUCTION

When piece of complex geometry is nitrided by plasma produced by direct current (DCPN), effects such as overheating, electric arcs and irregular layer occur, making the process impracticable. In order to avoid this undesirable effect, solutions such as pulsed voltage source (PPN) and cathodic cage discharge (CCPN) are being presented as alternatives [1-3]. With the voltage source pulsed, effects are avoided by controlling pulse width (ton) and pulse repetition time (toff). In the discharge by cathodic cage the control is realized by the electrical shielding of the sample, thus avoiding the direct bombardment of the ions on its surface [4]. However, by modifying these sources, it will also modify the plasma species, which interfere with the kinetics of nitriding [1]. The population intensity of the plasma species in the PPN configuration will depend on ton and toff because each species has its own population growth. In general, plasma species have a lifetime higher than 100 μs [5], meaning that for toff greater than this value, all species are in the process of recombination when the next pulse begins. Thus, by adjusting these times, the kinetics of nitriding can be modified. In the case of CCPN, the species that reach the sample surface are those generated by hollow cathode in the wall of the cage and, therefore, different from those in the DCPN. Thus, if the three plasma configurations are used to nitrate similar surfaces, even at the same treatment time and temperature, it is expected that there will be difference in layer formation kinetics. It is known that the nitrided layer is formed by a zone of compounds and another zone of diffusion. Mechanical properties of the surface are sensitive to the relative thicknesses of Fe_4N-γ 'and $Fe_{2-3}N$-ε phases in the compound zone [6,7]. In the present work, the physical and microstructural characteristics of the nitrided layers formed on AISI 1045 steel surfaces, treated in the configurations DCPN, PPN or CCPN were comparatively investigated.

2. MATERIALS AND METHODS

In this study, AISI 1045 steel disks, dimensions 5.4 mm x 3.0 mm (diameter x thickness) were used. The samples were prepared metallographically until polishing with alumina 0.05 μm. They were then cleaned

Clodomiro Alves Junior: Clodomiro Alves Junior Received on: 26/11/2018 Accepted on: 09/03/2019

10.1590/S1517-707620190002.0686

with acetone under ultrasonic stirring for 10 minutes. All treatments were carried out in the same bell-type reactor (Figure 1a), consisting of a cylindrical stainless steel tube 50 cm x 32 cm (height x diameter). The walls of the reactor were grounded, constituting the anode. Three configurations were used for plasma nitriding, namely: plasma nitriding with DC voltage (DCPN), pulsed voltage (PPN) and cathodic cage (CCPN). The difference between the DCPN and PPN configuration is that in the latter the voltage is pulsed (Figure 1b). For the CCPN configuration, the sample was placed inside a cage (Figure 1c). The cathodic cage was constructed in AISI 304 stainless steel tube, with dimensions of 35 x 50 mm (height x outer diameter), with 3 mm wall thickness. A disk of 50.0 mm x 1.0 mm (diameter x thickness) was placed on the tube, with 8 equidistant holes and a diameter of 7.6 mm.

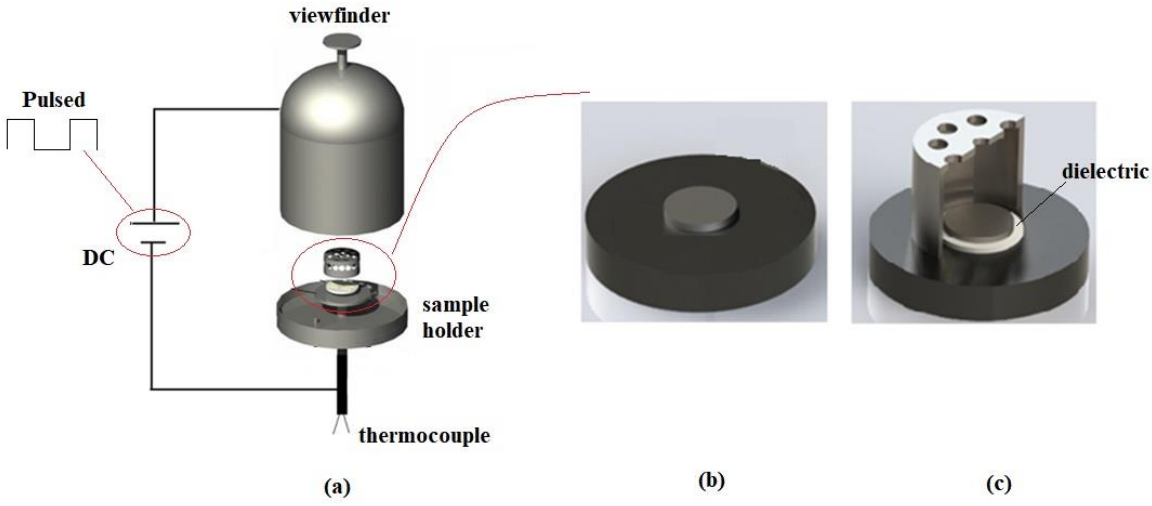

Figure 1: (a) Illustration of the reactor and positioning of samples during nitriding; (b) DCPN and PPN configurations; (c) CCPN configuration

Before each treatment, cleaning was performed using a flow rate of 20 cm 3 / min, 50% Ar-50% H 2, temperature of 250 ° C and pressure of 1 mbar for 30 minutes. After cleaning, the treatment was followed, which was carried out in the same flow but 80% N_2 and 20% H_2 atmosphere. The treatment conditions for the three processes are shown in Table 1.

Table 1: Parâmetros utilizados no processo de nitretação a plasma

Parameter	DCPN	PPN	CCPN
Current (A)	0.36	0.42	0.43
Voltage (V)	700	828	680
Power (W)	252	173.88	292.4
Pulse (μs)	-	On: 150 Off:150	-
Time (h)	3	3	3
Temperature (° C)	450	450	450
Pressure (mbar)	2	2	2

After 3 hours of treatment, the source was turned off and the samples were cooled in the working atmosphere. The samples were characterized for crystalline phases, microstructure and microhardness. The phases of the nitrided layer were analyzed, as well as qualitatively estimated the thicknesses of the individual phases, using DRX with grazing incidence. Shimadzu diffractometer, model XRC-6000 with Cu-Kα radiation was used. For characterization with grazing incidence (GIXRD) was coupled THA-1101 device (Shimadzu-6000 XRC) for thin films. Angles of incidence of 0.5°, 3° and 20° and velocity of 2.0 degrees / min, for 2θ between 30^o and 92^o were used. By obtaining the ratio of the diffracted intensities of the planes of the phases ε and γ ', the relative thicknesses (x_ε /$x_{\gamma'}$) were estimated at different depths. By observing the diffractograms for progressive angles of grazing incidence, it is possible to verify which phases are present for the

depth of the respective angle. It is also possible to verify the order of growth of the layers from the substrate, even if there was growth in some preferential orientation [9].

For microstructural analysis the Nikon Elipse MA 100 optical microscope coupled to a Nikon Digital Seght DS camera were used. Image analysis and processing were performed with free software Image J.

Chemical attack for microstructural development was performed with Nital 2%. Surface microhardness tests were performed with a Shimadzu, HM model 10gf (98.07 mN-HV 0.01) load for 10 s with seven measurements in each region.

3. RESULTS

Figure 2 shows micrograph of the profile of the nitrided layer (2a) and the respective diffractograms for angles of incidence of 0.5°, 3° and 20° (figure 2b). The JCPDS card 00-003-0925 (Fe4N) and 00-006-0627 (Fe2-3N) were used for indexing the diffractograms.

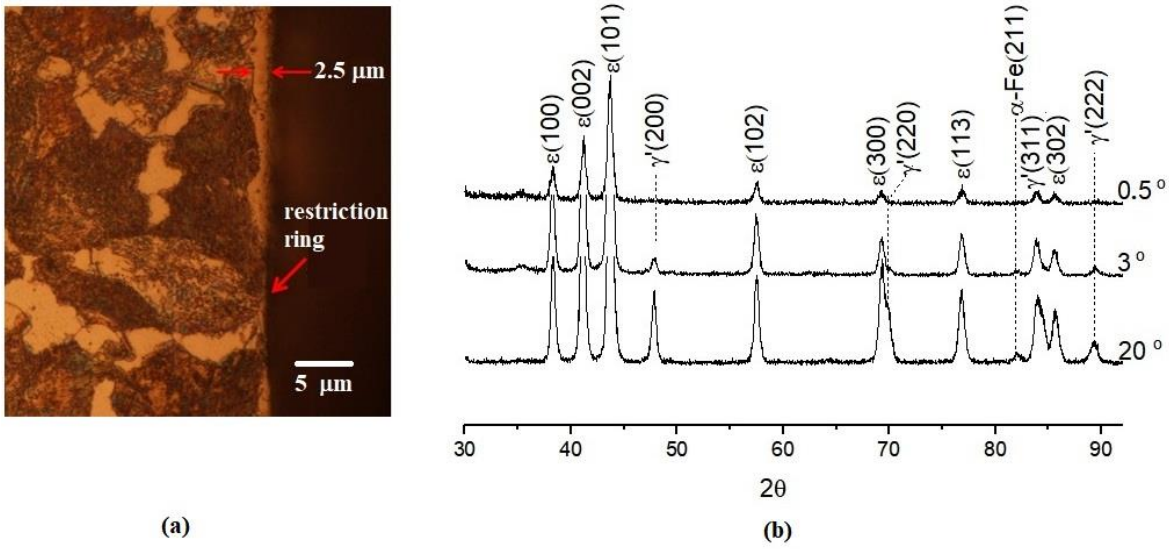

Figure 2: (a) Profile micrograph of the nitrided layer and (b) diffractograms for 0.5°, 3° and 20° incidence angles of the nitrided sample with DC source.

When using 0.5° incidence, only peaks referring to the ε-$Fe_{2-3}N$ phase were observed, where the most intense peak was ε (101), at 43.64°, indicating that the outermost layer is monophasic and formed by $Fe_{2-3}N$ phase. It is known from the Fe-C-N phase diagram that for a rich mixture of C + N, phase ε is dominant [6]. In the case of the DCPN treatment, due to the longer sputtering time, there was a greater decarburization and, therefore, a higher amount of carbon in the atmosphere favoring the ε phase formation. Upon observing an incidence of greater depth, such as the angle of 3°, the peak γ '(200) appears, which is the most intense of the phase γ'-Fe4N. The intensity of the diffraction peak for this phase is further increased for the 20° angle of incidence. It is also possible to observe the appearance of the substrate phase, Fe-α phase, indexed by the datasheet JCPDS 00-087-0721. Therefore, it can be stated that the radiation for the angle of incidence of 20° completely crossed the layer corresponding to the phase γ'-Fe4N. To estimate the ratio x_ε / $x_{\gamma'}$, the total thickness of the zone of compounds ($x_\varepsilon + x_{\gamma'} = 5$ µm) was also taken into account. The ratio $I_{\gamma'}(200) / I_\varepsilon (101)$ was 0.026 and 0.163 for 3° and 20°, respectively. It is also possible to observe the decrease of the layer in the vicinity of the edge (Figure 2a) caused by edges effects of the DCPN configuration. The disappearance of the layer was total for 2 mm of distance from edge.

Profile nitrided layer (Figure 3a) and glazing incidence diffractograms (Figure 3b) for samples nitrided by PPN. Like the DCPN, only peaks corresponding to the ε-$Fe_{2-3}N$ phase were observed with 0.5° incidence angle, meaning that this is also the outermost phase of the nitrided layer. At higher angles of incidence, 3° and 20° the γ'- phase appears, whose peaks increase the intensity as the depth of penetration of the radiation increases. Comparing the variation of the peaks of the γ' phase, it is verified that its relative intensity, mainly for angle of 20°, is greater than in the DCPN. This result suggests that the longer sputtering time on the sample surface contributed to the formation of the ε phase due to the greater decarburization of the surface.

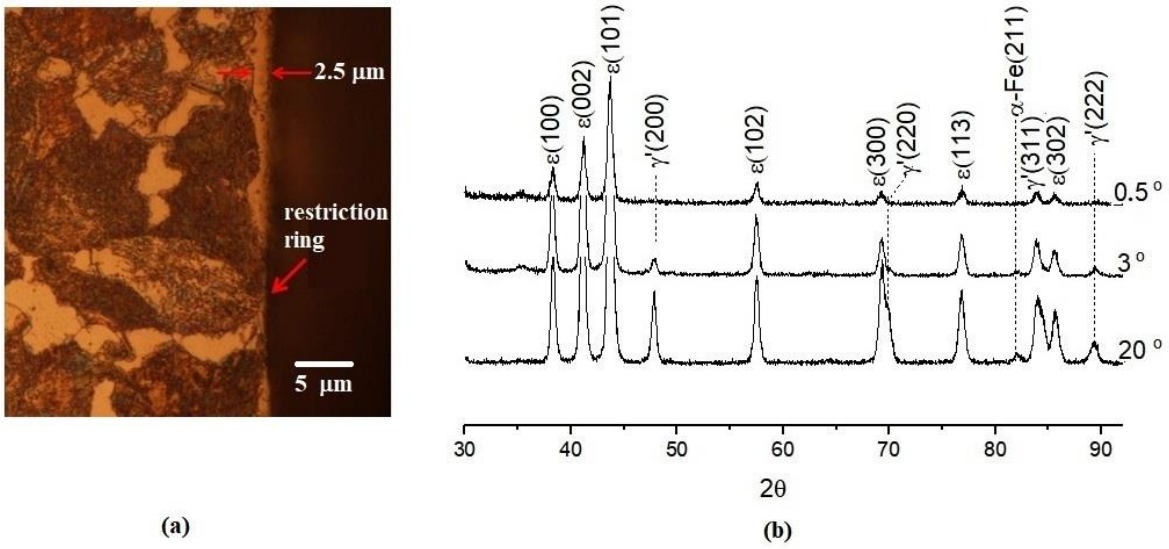

Figura 3: (a) Cross-section micrograph of nitrided layer by pulsed voltage source showing the reduction in restriction ring and (b) grazing incidence X-ray diffraction patterns for incident angles at 0.5°, 3° and 20°.

Reduction of the layer due to the edge effect is observed but less intense than in the DCPN (Figure 3a). This can be justified because at the pulsed voltage, when the source is switched off (toff), high concentrations of ions present at the edges are undone, reducing the shielding by the ions reflected near the edges [3]. The ratio $I_{\gamma'}(200)$ /$I_{\varepsilon}(101)$ was 0.38, for incidence of 20°, meaning less thickness of the ε phase than in the DCPN. It is possible to observe the micrograph of the profile of the layer in the vicinity of the edge (Figure 3b), it is possible to notice the decrease of the thickness caused by edge effects typical of the DCPN configuration. The disappearance of the layer was total for distance of 2 mm from the edge.

For samples nitrided by CCPN (Figure 4), the microstructure differs completely from the previous ones (DCPN and PPN). By the diffractogram with incidence of 0.5° it is possible to verify the formation of a biphasic layer on the surface, composed of the phases γ 'and ε. Note also, through the 3° and 20° diffractograms, that the phase ε reduces drastically with depth, compared to previous processes. Our justification for this is that in the CCPN, unlike the other processes, there is no ion collision and subsegmental formation of metastable compounds. In this case the nitriding process is totally controlled by diffusion, as in the gas nitriding process, except for the atmosphere, composed of energy particles, which is easily adsorbed on the surface. The presence of nitrides in the grain boundaries of nitrided samples (Figure 4a) corroborates our hypothesis.

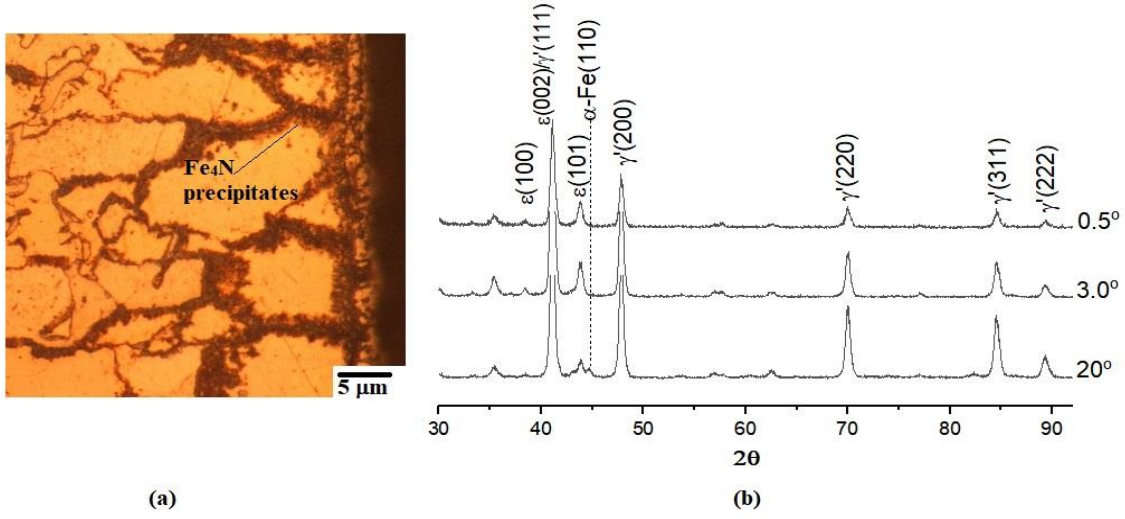

Figure 4: (a) Profile micrograph of the nitrided layer treated by CCPN and (b) Diffractogram of the surface of the nitrided sample.

A comparison between the intensity diffracted by the γ' (200) plane and the ε (101) or ε (102) plane, for a grazing incidence angle of 20°, is presented in table 2. It can be observed that the greatest thickness of the ε- phase was in the DCPN, followed by the PPN and the minor in the CCPN. This same order can be attributed from more energetic to less energetic character of the plasma. In DCPN the ions are continually colliding with the surface of the sample, creating defects, forming unstable compounds and sputtering more atoms. In PPN, despite the existence of the same effects of DCPN, these are diminished by the cut of the voltage (t_{off}). Differently from these two processes, CCPN has no ion collisions on the sample surface. Although the atmosphere is also composed of ions, they are not accelerated to the surface of the sample. They are adsorbed on the surface more easily than in gaseous nitriding. In addition, metal atoms stripped by sputtering from the cathodic cage produce metallic nitrides on the surface.

Table 2: Ratio of diffracted intensity of plane γ'(200) and plane ε (101) or ε (102), using incidence angle of 20°.

	DCPN	PPN	CCPN
$I_{\gamma'}(200)/I_{\varepsilon}(101)$	0,16	0,38	11,40
$I_{\gamma'}(200)/I_{\varepsilon}(102)$	0,83	2,02	39,71

Comparing the microhardness values on the surface of the samples (Figure 4), it is noted that the DCPN and PPN produced samples with very close hardness, except that in the PPN the hardness is more uniform.

The lower value of the hardness at the edges is associated with the appearance of the restriction ring produced by the edge effect. This shows that in the DCPN sample the edge effect was more intense than in the other treatments, which obtained a more uniform microhardness from the edge to the center. No microhardness variations between edge and center were detected in the sample treated by CCPN. This result agrees with previous studies in other steels [1, 10, 11]. The CCPN sample had a lower microhardness compared with the DCPN and PPN treatments, probably due to the lower thickness of the composite layer.

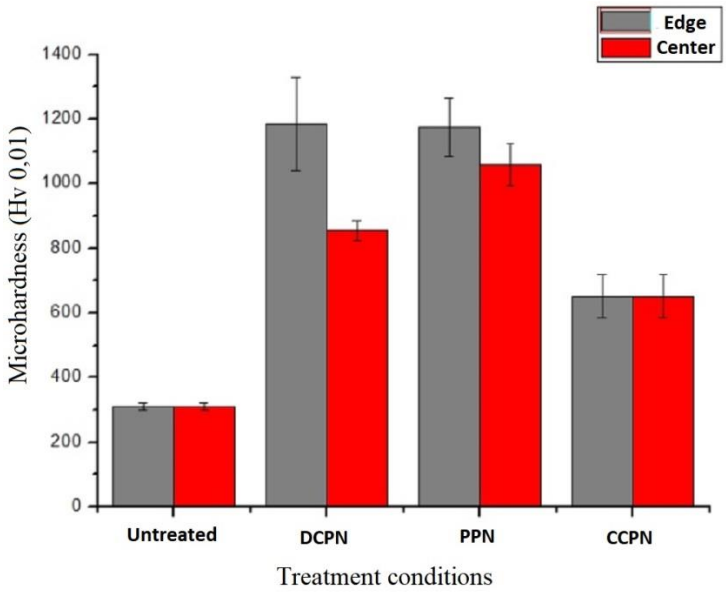

Figure 5: Surface microhardness value of nitrided samples.

4. DISCUSSION

When parts are treated by DC voltage, ions are continuously accelerated to the surface, colliding and producing different events. Among these events are sputtering, heating, defect production and surface metastable reactions. However, in parts with complex geometry, especially in regions that have sharp points, corners, holes and / or sharp edges, there are constraints that are strongly dependent on the intensity and uniformity of the electric field (Figure 6).

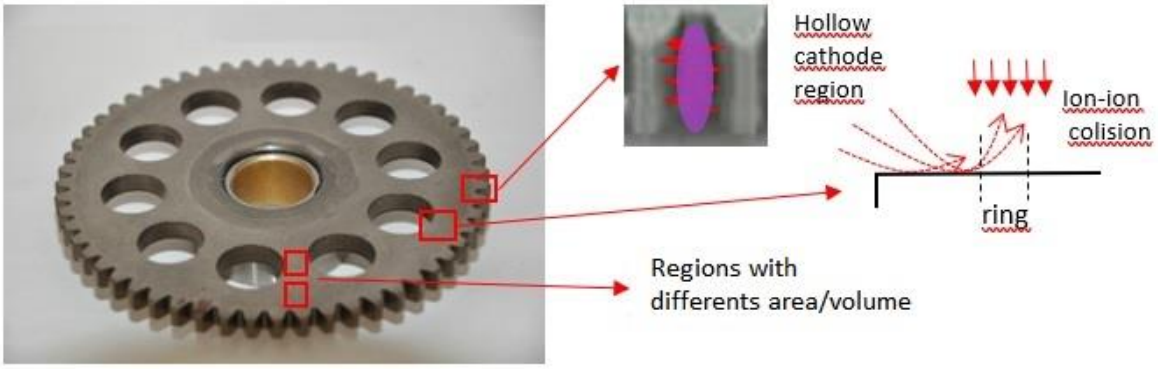

Figure 6: Undesirable effects occurring during plasma nitriding of parts with complex geometry.

The charge density, q, for corners, flat surfaces and edges, is given by the following Laplace equations (3).

$$q(r) = kr \quad \text{(corner)} \tag{1}$$

$$q(r) = k \quad \text{(flat surface)} \tag{2}$$

$$q(r) = kr^{-1} \quad \text{(edge)} \tag{3}$$

Where k is a coefficient which depends on the induction potential and r is the distance from the edge (or corner). As a result of these charge irregularities and, consequently, of the electric field and potential, the bombardment conditions vary along the work piece and affect the balance of the kinetic energy and the nitriding process on the surface. Equations 1-3 show that in small parts, where the presence of edges is significant, such as gears, molds, and needle punched parts are strongly affected by this effect, leading to irregular formation of nitrided layers and high variation in surface hardness [3]. As the samples are at high cathodic potential, in which the plasma acts directly on them, there are distortions of the electric field around its edges and corners, affecting the distribution and ion flow of these regions, this can cause the appearance of the hollow cathode effect, non-uniformity in temperature and arcing [2].

In the example of figure 6 the effect of hollow cathode between the teeth of the gear can be verified. Electrons in this region perform a zig-zag movement due to the repulsive potential of the two inner walls. This increases the ion density and, consequently, higher heating due to the increase in the number of collisions in these walls. This effect is called the hollow cathode. It is also possible to observe the edge effect that results in the formation of regions that are poor in ring nitriding. This happens because in the vicinity of the edge the electric field changes its direction, forcing the ions to collide in different angles of incidence. These ions to the reflecting surface, ions collide with a front impact, preventing sputtering in a particular region (ring) and thus the effects of plasma-surface interactions are less intense or absent. Differential heating is also shown in figure 6. It is observed that for regions between the two holes there is a higher incidence of ions (collisions on the upper and lateral surfaces) than in the peripheral region (collision only on the upper surface), implying higher heating in the first region, with greater area / volume ratios. Since the samples used in the present work were flat surface and disc-shaped, hollow cathode effect was not expected in the DCPN.

However, at distance of 2 mm from the edge, a ring with a thickness about 10 μm (restriction ring) was formed. This effect occurs because in the edge the charge density, and therefore equipotential surfaces, is given by equation 3. Since the electric field is always perpendicular to the equipotential surfaces, ions near edge collide on surface with different angle. When reflecting they collide with other ions that are perpendicular to the surface. The result of this collision is the depletion of ions in a particular region (constraint ring), as shown in Figure 6.

It can be observed (Figure 2a) that there was almost complete disappearance of the nitrided layer in this region. This effect was less pronounced in the PPN configuration, where the thickness had only small reduction in this region. This can be explained by the change in charge densities predicted by the Laplace equations. As the applied voltage is pulsed, the load distribution behaves as in the DCPN configuration during the connected pulse and disperses, tending to the recombination of the loads, during the off time. This explains the less severe character of the edge effect, as well as the surface sputtering. It was observed that in the DCPN there was a greater thickness of the ε-$Fe_{2-3}N$ phase. It is known from the Fe-C-N phase diagram that this phase is stable for higher concentrations of N + C in the atmosphere [6]. As the concentration of N_2

used in the nitriding atmosphere in these two configurations was the same, it can be concluded that the increase in concentration was due to the decarburizing of the sample. The higher time of ion-surface collision of the DCPN than in the PPN, promoted greater extraction of C atoms by sputtering, thus justifying the greater thickness of the ε phase in the DCPN. This hypothesis was more evident when the surface of the CCPN samples was observed. In this configuration there is no attractive potential of the ions to the surface of the sample and therefore there is no sputtering. This way there will be no decarburization of the surface. In fact, the peaks referents to the ε phase are very small, even for incidence angles of 0.5^{o}, which reinforces our hypothesis.

5. CONCLUSIONS

Two alternative methods of plasma nitriding were compared with the conventional continuous voltage plasma nitriding process. The three methods showed to be effective in modifying the surface, but different in the microstructure and hardness of the layer. It was verified that the DCPN and PPN treatments presented layers with a higher thickness of the ε-$Fe_{2-3}N$ phase, which were justified by the presence of carbon in the atmosphere, resulting from sputtering decarburization of the steel surface. The greater presence of this phase in the CCPN than in the PPN corroborates our hypothesis. With respect to the edge effect (presence of restriction rings), it was found that the PPN is lower than DCPN while the CCPN it was completely eliminated. However, samples nitrided by CCPN presented lower layer thickness, lower surface hardness and diffusion in grain contours. This result can be justified by the inexistence of surface sputtering, where the process must be mainly controlled by diffusion, as in the gas nitriding process. That is, unlike the other processes, in the CCPN the zone of compounds is formed after saturation of the matrix.

6. ACKNOWLEDGMENTS

This project was funded by the National Council for Scientific and Technological Development (CNPq) and the Coordination of Higher Education Personnel Training (CAPES).

7. BIBLIOGRAPHY

[1] SOUSA, R. R. M., *et al*., "Nitriding of AISI 1020 Steel: Comparison Between Conventional Nitriding and Nitriding with Cathodic Cage", Materials Research, v. 17, n. 3, pp.708-713, 2014. URL: http://www.scielo.br/scielo.php?script=sci_arttext&pid=S1516-14392014000300024

[2] ALVES JR, C., *et al*., "Effect of workpiece geometry on the uniformity of nitrided layers", Surface Coatings and Technology, v, 139, pp. 1–5, 2001.

[3] ATAIDE, A.R.P., *et al*., "Effects during plasma nitriding of shaped materials of different sizes", Surface, Coatings and Technology, v.167, 52-58, pp. 52–58, 2003.

[4] ALVES JUNIOR, C., *et al*., "Comparison of Plasma-Assisted Nitriding Techniques" , In: Encyclopedia of Tribology**,** New York, Springer, v. 716, p.1-7, abr. 2013. URL: https://link.springer.com/referenceworkentry/10.1007%2F978-0-387-92897-5_716

[5] HORIKAWA, Y., *et al*. "Lifetime of Molecular Nitrogen at Metastable $A^{3}\Sigma_{\upsilon}^{+}$ State in afterglow of inductively-coupled nitrogen plasma, Japanese Journal of Applied Physics, v.51, pp. 126301- 1263015, 2012.

[6] JACK, K.H., "Binary and ternary interstitial alloys I e II.- the Fe-C-N system" Proceedings of Royal Society A, v. 195, pp.41-55, 1948. URL: https://www.jstor.org/stable/98301?seq=1#page_scan_tab_contents

[7] SUN, Y., BELL, T. "Plasma surface engineering of low alloy steel", Materials Science and Engineering, v.140, pp. 419-434, july, 1991. URL: https://www.sciencedirect.com/science/article/abs/pii/092150939190458Y

[8] BOUROUSHIAN, M., KOSANOVIC, T. "Characterization of Thin Films by Low Incidence X-Ray Diffraction", Crystal Structure Theory and Applications, v.1, pp. 35-39, 2012. URL: https://file.scirp.org/pdf/CSTA20120300004_13707060.pdf

[9] ALVES JÚNIOR, C., *et al*., "Caracterização de camadas nitretadas de aços AISI-409, utilizando a técnica de difratometria de raios-x." 50^{o} Congresso Anual da ABM**,** São Paulo, v. 5, pp. 271-278, ago. 1995.

[10] ALVES JR. C., *et al*., "Use of cathodic cage in plasma nitriding", Surface and Coatings Technology**,** v. 201, n. 6, p.2450-2454, dezembro. 2006. URL: https://www.researchgate.net/publication/229369352_Use_of_cathodic_cage_in_plasma_nitriding

[11] RIBEIRO, K. J. B., *et al*., "Industrial application of AISI 4340 steels treated in cathodic cage plasma nitriding technique", *Materials Science And Engineering: A*, v. 479, n. 1-2, pp.142-147, 2008. URL: https://www.sciencedirect.com/science/article/abs/pii/S0921509307013317

ORCID

Priscila Borges https://orcid.org/0000 - 0002-7489-6079
Nathalia Freitas https://orcid.org/0000-0002-1825-1647
Jussier Vitoriano https://orcid.org/0000-0002-9357-2088
Clodomiro Alves https://orcid.org/0000-0002-5547-5922